Lithuanian Journal of Physics, Vol. 53, No. 1, pp. 1–16 (2013)

TRACING COHERENCES OF QUANTUM STATES BY ULTRAFAST LASER SPECTROSCOPY

E. Gaižauskas [a] and G. Trinkūnas [b]

[a] *Laser Research Center, Vilnius University, Saulėtekio 10, LT-10222 Vilnius, Lithuania*
[b] *Center for Physical Sciences and Technology, Savanorių 231, LT-02300 Vilnius, Lithuania*
E-mail: eugenijus.gaizauskas@ff.vu.lt

Received 3 December 2012; accepted 22 December 2012

An overview of the influence of coherent coupling in light–matter interaction traced by transients in pump-probe spectroscopy is given, with special emphasis on interest and works provided by the authors. Advantages of this technique used to trace pathways of transfer and decay of quantum coherences in atoms, molecular aggregates, and biological structures, as well as feasibility of the probing of both the lifetime and characteristic lengths (area, volume) of coherent excitations are discussed. Theoretical analysis of the pump-probe measurements is based on the numerical solution of the equation for the reduced density matrix in the representation of atomic, molecular, and excitonic states, considering coherent coupling between light and appropriate quantum states precisely.

Keywords: ultrafast laser spectroscopy, molecular aggregates, quantum coherences

PACS: 78.47.jh,78.47.nj,71.35.-y

1. Introduction

Ultrafast pump-probe laser spectroscopy is defined as a study of molecules on extremely short time scales (from nanoseconds to femtoseconds) after their excitation with a pump-laser pulse. Among many different procedures developed at the very beginning of the "laser era", ultrafast transient four-wave mixing (FWM) based methods were used to trace decays of excited states in atoms, molecules, and molecular aggregates whose reaction to light was of interest [1].

Coherent effects arising during resonant matter interactions with ultrashort laser pulses have been observed in some of early (pump-probe type) experiments and were used to be called "artifacts". Usually, these effects happen as long as used durations τ_L, τ_P of the pump and probe pulses are long, as compared to the relaxation time T_2 of induced polarization (coherence). On the other hand, the lifetime of the coherence of excited quantum states has become the subject of intensive studies over recent years due to their multiple potential applications, ranging from laser cooling to isotope separation, generation of giant pulses of the laser light in a short-wavelength region [2], tailoring material dispersion [3–5].

Besides, nowadays coherent interaction in many-level quantum systems gives promising concepts towards practical realization of quantum information processing [6–8]. Among the main challenges which affect progress in this field, the control of the lifetime of created quantum state coherence should be emphasized. Additionally, recent two-dimensional (2D) photon echo experiments on light harvesting systems suggest that excitation energy transfer in these systems occurs coherently rather than by incoherent hopping [9]. Such findings raise questions about the role and significance of quantum coherences in the light harvesting efficiency [10–15]. All these necessitate an increasing demand both for the new structures with distinct coherence lifetime, methods for the characterization of quantum states, and adequate treatment (description) of the coherent light–matter interaction, including transfer of coherences in complex quantum systems.

It should be stressed that a long lifetime of coherences leads to significant changes in the spatial and temporal evolution of the excited states in molecular aggregates (e. g. due to the annihilation of excitations) and modifies the response of the media to the probe field by the ac Stark shifts as well as power broadening in case of strong excitation. This implies importance of the non-perturbative treatment of light–matter interaction in many experimental situations, whereas common treatment of ultrafast FWM experiments is based on the perturbative (in the field–matter interaction) theory placing special emphasis on quantum system – bath interaction. Specifically, treatment by Mukamel and co-workers [1, 16, 17], well known as a dynamical model of multiple Brownian oscillators (MBO), is widely used for the analysis of the relaxation induced by the solute–solvent interaction in the femtosecond FWM spectroscopy.

On the other hand, modern experimental methods of laser spectroscopy provide one with reliable parameters both of vibrational modes, playing the major role in dissipation process, and their relaxation rates. Therefore, when learning about the excitation dissipation processes, it is a natural way to explore these new parameters (rate constants) rather than use bath correlation functions, estimation of which is based either on the stationary spectra measurements or on a complex fitting of the experimental data as obtained by means of different modifications of the FWM experiments. In general, the disadvantage of simulation of the time-dependent behaviour of the solvation process within the stochastic (e. g. MBO) model is that in this case not only potentially *useful information can be lost*, but also *many useful experimentally provided information cannot be used*, if the solvent is not described in terms of microscopic quantities.

Motivated by experimental investigations of the ultrafast excited state relaxation and transfer in artificial molecular aggregates, light-harvesting antennas and natural photosynthetic systems, the Redfield theory of relaxation was used as an approach for the nonperturbative quantum dynamics description of molecular excitonic systems. The method proved to be an efficient approach for simulation and tracking coherences and energy transfer dynamics in complex molecular systems. Specifically, it has been used to simulate ultrafast pump-probe measurements, stressing applications of the method to light and matter interaction in several models. Starting with simple two- and three-level atoms and progressing to many-level systems, this paper attempts to stress the significance and measurement possibilities of coherent electronic excitation relaxation, exciton–exciton annihilation and transfer phenomena, as well as possibilities to characterize lifetimes and pathways of this transfer in complex molecular systems.

2. Background of nonperturbative description of pump-probe spectroscopy

The light-induced changes in many-level systems can be described by the density matrix, which is governed by the following Liouville equation:

$$\frac{\partial\hat{\rho}}{\partial t} = [\hat{\rho}, \hat{H}_0 + \hat{H}_{\text{int}}] + \left\{\frac{\partial\hat{\rho}}{\partial t}\right\}_{\text{rel}}, \tag{1}$$

where the total Hamiltonian is divided into its unperturbed part H_0 of the ground and excited states of the system under consideration with electronic and vibrational energy states and perturbation term H_{int} related to the external electric fields. The last term in Eq. (1) accounts for the complexity of the relaxation processes and might be approximated by means of the Redfield relaxation operator $\hat{\Re}$ [18], i. e.:

$$\left\{\frac{\partial\hat{\rho}}{\partial t}\right\}_{\text{rel}} = -\hat{\Re}\rho. \tag{2}$$

In order to follow the evolution of excitation in the system, the basic set of functions, which for independent modes are simple products of the corresponding wave functions, might be used for representation of the density matrix. For the sake of simplicity in describing the corresponding equations we will apply a single (combined) index for excitations in different electronic bands (by assuming e. g. $|j\rangle \equiv |j_1, j_2, \ldots\rangle$).

Expanding the density matrix operator with respect to the basis of the wave functions described above, $\hat{\rho} = \sum_{i,j} \rho_{ij} |i\rangle\langle j|$, the matrix element ρ_{ij} is defined, where according to our definition i and j enumerate quantum states in different electronic bands. The Hamiltonian of the system under consideration and the interaction with the external field by means of the same representation can be determined as follows:

$$\hat{H}_0 = \sum_i \in_i |i\rangle\langle i|, \quad \hat{H}_{\text{int}} = -\sum_{i,j} \mu_{ij} |j\rangle\langle i| E, \qquad (3)$$

where $\mu_{ij} = d\langle j| i\rangle$is the corresponding transition dipole moment between the eigenstates in different electronic manifolds.

At this point we recall some points of the well-known pump-probe spectroscopy method. Usually, fields are directed to the sample at different angles (see Fig. 1). The absorption changes are detected by a probe field (having mean frequency ω_{P} and a wave vector $\mathbf{k}_{\text{P}}$), after the system is exposed to the laser (pump) pulse characterized by frequency ω_{L} and wave vector $\mathbf{k}_{\text{L}}$. Thus, we write the electric field as a superposition of both quasi-monochromatic plane-wave pulses:

$$E(t) = \frac{1}{2}\left[\mathcal{E}_{\text{L}} e^{i\mathbf{k}_{\text{L}}\mathbf{r} - i\omega_{\text{L}}t} + \mathcal{E}_{\text{P}} e^{i\mathbf{k}_{\text{P}}\mathbf{r} - i\omega_{\text{P}}t} + \text{c.c.}\right], \qquad (4)$$

where $\mathfrak{E}_i(t)$ (i = L, P) are the slowly varying complex electric field envelopes, and c.c. denotes the complex-conjugate terms. The frequencies of the pump and probe pulses are considered being close the resonance of the optical transitions of the system, i. e. when inequality $\hbar|\Delta_{ij}^{\text{L}}| = |\in_i - \in_j - \hbar\omega_{\text{L}}| << |\in_i - \in_j|$ is fulfilled. Therefore, the rotating wave approximation [19] can be applied to specific models, giving equations for the material variables [20, 21]. In both perturbative and nonperturbative treatment of the material equations, spectroscopic signals have to be distinguished via the direction of wave vectors. The perturbative (up to the third order in the field–matter interaction) approach allows one to separate terms with proper wave vectors [1, 17], whereas the nonperturbative one is based on the solution of a set of differential equations for material variables (coherences and populations) with the specific wave vectors. Thus, for the diagonal density matrix elements (populations) we use the expansion

$$\rho_{ii} = \sum_{m=-1,0,1} \rho_{ii}^{m} e^{im\mathbf{h}\mathbf{r}}, \qquad (5)$$

where $\mathbf{h} = |\mathbf{k}_{\text{L}} - \mathbf{k}_{\text{P}}|$ in a k-space. Additionally, expansions of the nondiagonal matrix $i \neq j$ elements (polarizations) read:

$$\rho_{ij} = \rho_{ij}^{\text{L}} e^{i\mathbf{k}_{\text{L}}\mathbf{r}} + \rho_{12}^{\text{P}} e^{i\mathbf{k}_{\text{P}}\mathbf{r}} + \rho_{ij}^{\text{L2P}} e^{i(2\mathbf{k}_{\text{L}}\mathbf{r} - \mathbf{k}_{\text{P}}\mathbf{r})}. \qquad (6)$$

Further, in our simulations it is assumed that the moduli of wave-vectors $|\mathbf{k}_{\text{L}}| \approx |\mathbf{k}_{\text{P}}|$ and that modulation of the refraction index is quite small. Therefore, in Eqs. (5) and (6) we restricted us to the first order of diffraction.

Before concluding this section, some important aspects on the description of the relaxation processes should be discussed. In general, the Redfield relaxation tensor is defined by the stationary correlation functions of the system-bath coupling operator [18, 22]:

$$\Re_{ij}^{kl} = \Gamma_{l,j,i,k}^{+} + \Gamma_{l,j,i,k}^{-} - \delta_{l,j}\sum_r \Gamma_{i,r,r,k}^{+} - \delta_{i,k}\sum_r \Gamma_{l,r,r,j}^{-}, \qquad (7)$$

where:

$$\Gamma_{l,j,i,k}^{+} = \frac{1}{\hbar}\int_0^\infty dt e^{-i\omega_{i,k}t}\langle V_{l,j}(t) V_{i,k}(0)\rangle, \qquad (8a)$$

$$\Gamma_{l,j,i,k}^{-} = \frac{1}{\hbar}\int_0^\infty dt e^{-i\omega_{l,j}t}\langle V_{l,j}(0) V_{i,k}(t)\rangle, \qquad (8b)$$

$V_{i,j}(t)$ being the matrix element of the system–bath coupling operator between eigenstates $|i\rangle$ and $|j\rangle$ of the system in the interaction representation, $\langle ...\rangle$ represents the trace over the bath in thermal equilibrium, and $\hbar\omega_{ij} = \in_i - \in_j$. As it follows from Eq. (8), for the defined model of the system-bath coupling the Redfield tensor elements can be estimated, in principle, from the stationary spectra. Specifically, when using a harmonic oscillator model as a bath Hamiltonian, all effects induced by electron coupling to the vibrational modes may be incorporated through the line broadening function [1].

On the other hand, in particular cases the rate constants $\Re_{ij}^{kl}$ $(i = k, j = l)$ of population relaxation

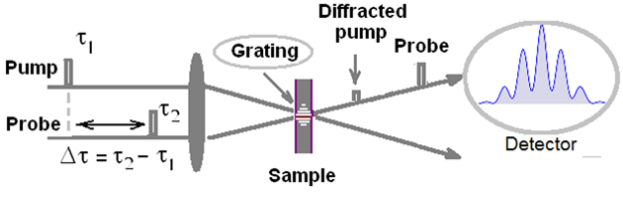

Fig. 1. General scheme for a pump-probe experiment. A case of the negative time delay, when a relatively strong laser pulse passes the sample after the probe and self-diffracts on the created grating. Spectra detected at the probe direction exhibit an oscillatory feature with characteristic modulation frequency $\Delta\tau$, resulted from two maxima in time-dependence of the signal.

might be taken directly from the existing experimental data [23, 24] or chosen as fitting parameters of the experimental and theoretical data. We will follow throughout this paper the former (dynamical) way and will not specify here the coupling operator (as well as the bath Hamiltonian) explicitly. According to our notations $\Re_{ij}^{kl}$ $(i = j,\ k = l)$ determines the dephasing, and $\Re_{ij}^{kl}$ $(k, l \neq i, j)$ the coherence transfer [18, 25, 26].

3. Coherence signatures of transient spectroscopy

3.1. Pump-probe spectroscopy in two-level approximation

The main disadvantage (shortcoming) of using the Redfield relaxation theory is that some (non-Markovian) features of pump-probe experiments cannot be fitted within this description, because it is based on the assumption that the mean correlation time τ_c of the system–bath interaction is much shorter than the time scale under investigation. However, nowadays computational capacities make it possible to resolve the problems by introducing e. g. the noise function into the Hamiltonian (3) of the system and using repetitive calculations to find the averaged behaviour of the quantum system.

As an example, in this subsection we demonstrate that the spectral drift of pure non-Markovian nature may be observable in the difference absorption spectra (DAS) of the two-level quantum system (2LQS) resulting from the system-bath interaction. Specifically, we investigate the solute–solvent interaction by means of numerical analysis based on a stochastic model of 2LQS spectra.

Considering a simple 2LQS in the framework as described above in the previous section, we arrive at following equations (see [20, 27–29]) for material variables (polarization and population):

$$\frac{\partial}{\partial t} n_0 = i\Lambda_{\mathrm{L}} \rho_{12}^{\mathrm{L}} - i\Lambda_{\mathrm{L}}^{*} \rho_{12}^{\mathrm{L}^*} + i\Lambda_{\mathrm{P}} \rho_{12}^{\mathrm{P}} - i\Lambda_{\mathrm{P}}^{*} \rho_{12}^{\mathrm{P}^*} - \frac{n_0 - n_0(0)}{T_1}, \tag{9a}$$

$$\frac{\partial}{\partial t} n_1 = i\,(-\Delta_{\mathrm{P12}} + \Delta_{\mathrm{L12}}) n_1 + i\Lambda_{\mathrm{L}} \rho_{12}^{\mathrm{P}} - i\Lambda_{\mathrm{P}} \rho_{12}^{\mathrm{L}^*} - i\Lambda_{\mathrm{L}} \rho_{12}^{\mathrm{L2P}} - \frac{n_1}{T_1}, \tag{9b}$$

$$\frac{\partial}{\partial t} \rho_{12}^{\mathrm{L}} = -i\Delta_{\mathrm{L12}} \rho_{12}^{\mathrm{L}} + \frac{1}{2} i\Lambda_{\mathrm{L}} n_0 + \frac{1}{2} i\Lambda_{P} n_{-1} - \frac{\rho_{12}^{\mathrm{L}}}{T_2}, \tag{9c}$$

$$\frac{\partial}{\partial t} \rho_{12}^{\mathrm{P}} = -i\Delta_{\mathrm{P12}} \rho_{12}^{\mathrm{P}} + \frac{1}{2} i\Lambda_{\mathrm{L}} n_1 + \frac{1}{2} i\Lambda_{\mathrm{P}} n_0 - \frac{\rho_{12}^{\mathrm{P}}}{T_2}, \tag{9d}$$

$$\frac{\partial}{\partial t} \rho_{12}^{\mathrm{L2P}} = -i\,(2\Delta_{\mathrm{L12}} - \Delta_{\mathrm{P12}}) \rho_{12}^{\mathrm{L2P}} + \frac{1}{2} i\Lambda_{\mathrm{L}} n_1 - \frac{\rho_{12}^{\mathrm{L2P}}}{T_2}, \tag{9e}$$

where $\Delta_{\mathrm{L12}} = \omega_{\mathrm{L}} - \omega_{12}$ and $\Delta_{\mathrm{P12}} = \omega_{\mathrm{P}} - \omega_{12}$ are detunings of the pump and probe pulses from resonance, $\Lambda_{\mathrm{L,P}}(t)$ denote time-dependent Rabi frequencies of pump and probe fields, and common notations T_1, T_2 are used here for relaxation times in the 2LQS (for populations and polarizations, respectively). In our simulations the spectrum of the probe pulse is considered a supercontinuum. In this case the detuning of the probe pulse is not crucial, and the differential absorption (transmission) spectrum (DAS) of the probe field can be written as follows:

$$\Delta A(\omega, \tau) \sim \left| \int \Lambda_{\mathrm{P}}(\tau) e^{-i\omega t} dt \right|^2 - \left| \int \Lambda_{\mathrm{P}}^{0}(\tau) e^{-i\omega t} dt \right|^2. \tag{10}$$

To discuss the non-Markovian properties of the system it was assumed that the transition frequency ω_{12} underlies a stochastic process, i. e. that the frequency detuning in Eq. (9) is modulated by the additive noise $\Delta(t)$, which is a stochastic process with a zero mean value

$$\langle \Delta(t) \Delta(t') \rangle = D \exp\left(\frac{-|t - t'|}{\tau_c}\right), \quad \langle \Delta(t) \rangle = 0, \tag{11}$$

where τ_c and D denote the correlation time and dispersion of the Ornstein-Uhlenbeck process, respectively. The reduction of the noise correlation time below the duration of the pulses simply leads to the case of white Markovian noise which can be described analytically by introducing proper phase relaxation time in Eq. (9).

The non-Markovian situation was considered by taking τ = 0.2 ps. In this case, the coherent part of the signal becomes increasingly important in the vicinity of time delay zero as it is seen from Fig. 2. The present bleaching was called in a number of papers (see e. g. [30]) as a "spectral hole burning", despite it does not represent any real changes in the spectral distribution of populations and simply displays the spectrum of the pump pulse, which is taken considerably narrower in comparison to the spectrum of the quantum system. The distinct feature of the DAS resulted from non-Markovian treatment is that contribution of the absorption and stimulated emission (ASE) exhibits here a delay time depenedent shift (see Fig. 2(b)). Actually, the "hole moves" in the spectral region of more than 20 nm, and this ASE contribution to the DAS (which is caused by level population affecting absorption and stimulated emission processes) behaves in the most way as compared to the Markovian case. This bleaching approaches its maximum in the vicinity of zero delay and falls down for positive delay times, thus producing a negative dip (in addition to that contributed from the coherent interactions) in the DAS. The observed effect can be explained when noting that definite phase relations of the induced macroscopic polarization with respect to the light field are responsible for the up- and down-action of the field to the population kinetic. On the other hand, no definite phase relations for the macroscopic polarization can be defined for the time period over which the non-Markovian polarization relaxation takes place.

3.2. From two- to three-level approximations

As we have seen from the analyzed example of a simple 2LQS, coherence manifests itself in spectral changes that in addition are also influenced by the system environment to a great extent, i. e. a correct inclusion of the quantum system – environment interaction is of exceptional importance. This problem, unfortunately, appears to be even more complicated due to the structural and spectral complexity of the molecular aggregates, whose reaction to light will be discussed below. Particularly, when studying molecular aggregates special attention to the manifestation of transitions from one- to two-exciton states has to be paid due to the two-photon resonance-enhanced FWM [31]. In this case the measured signal has to be taken into account with a larger precision, as long-lived material coherences from different transitions could, in principle, affect the relaxation of excitations in such systems as photosynthetic light harvesting complexes.

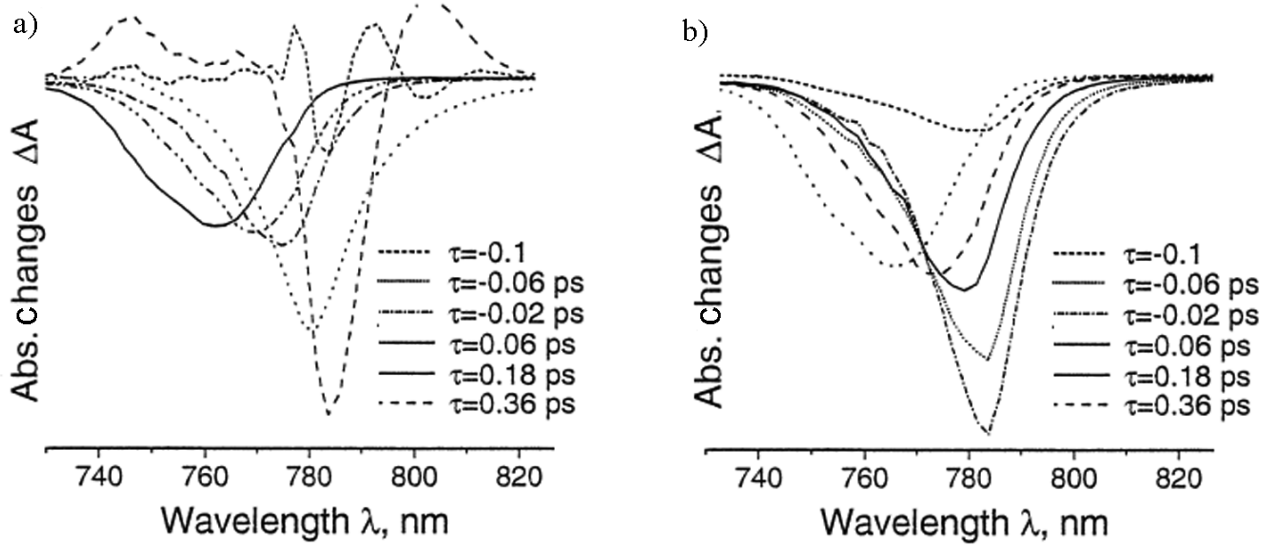

Fig. 2. (a) Time resolved total differential transmittance spectra for the 2LQS under non-Markovian relaxation conditions τ_c = 0.2 ps. (b) ASE contribution of the differential transmittance line shapes. Note the presence of the 'slow' drift of the spectral differences ('hole' in the spectra) towards the position of the system spectra as well as reduction of the signal for positive delay time.

Two-photon resonance-enhanced FWM processes taking place in circular aggregates were considered theoretically with respect to their influences on the pump-probe DAS [20], and remarkable changes of the signal spectra around the zero time delay arising from the two-photon resonance transitions to the two-exciton states has been discovered in this case. Time- and frequency-resolved pump-probe measurements in the vicinity of zero delay times have been shown to be sensitive to the manifestation of two-exciton states and, consequently, may be used for the analysis of the extent of exciton localization in the circular aggregates.

Note that many-level systems under two-photon resonance were studied in a number of papers [32–7]. Here, the main attention was paid to a three-level atom coherently excited by a two-photon resonant transition and *subsequently* driven by a weak field injected at one-photon resonance. A different situation, when the injected probe pulse appears prior to the pump, was not widely considered (except the cases of resonant femtosecond pump-probe spectroscopy [20]) even if such a sequence may have a considerable impact on coherent control over quantum states in a three-level system, as well as opens new possibilities of tracing realistic parameters in a macroscopic ensemble of states.

Recently, there has been demonstrated an experimental technique which provides a direct access to the dephasing times of coherences at different transitions in a three-level system [38] (as it is sketched in Fig. 3), when excited by a two-photon resonant pump and subsequently driven by a weak field injected at one-photon resonance. In the analysed case, in close analogue to the pump-probe spectroscopy measurements [20, 39], the role of the injected atomic coherence for a four-wave difference frequency mixing (FWDFM) process in a three-level quantum system (3LQS) with a two-photon pump was demonstrated. It was shown, specifically, that ultrafast dephasing of different coherences (excited states) can be detected from measurements of the intensity of the DFG signal as a function of probe delay for positive and negative delay times. These theoretical findings were supported by FWDFM efficiency measurements in K atomic vapours [38].

From the observed behaviour of the FWDFG efficiency in accordance with the interpretation given in [38] it could be stated that two-photon resonant enhanced FWM with a weak injected probe pulse represents a powerful tool for the spectroscopic studies of ultrafast processes and relaxation constants in molecular aggregates and photosynthetic antennas, where two-exciton states inevitably appear to be in the vicinity of two-photon resonance.

3.3. Theoretical modelling of early transients in femtosecond pump-probe spectra in a molecule

In what was described above we treated pure electronic two- and three-level systems. On the other hand, in molecules and molecular aggregates these (electronic) excitations often strongly couple to internal vibrational modes. Therefore, models which take into account nuclear degrees of freedom are of interest. Most of common models of theoretical descriptions from time resolved (femtosecond) spectroscopy of molecules are based on the MBO model and use perturbative treatment of field–matter interaction. Such a treatment, when applied to many-level systems, faces huge computational difficulties evaluating multiple integrals for actual Feynman graphs. Further, we demonstrate, how the treatment based on the numerical

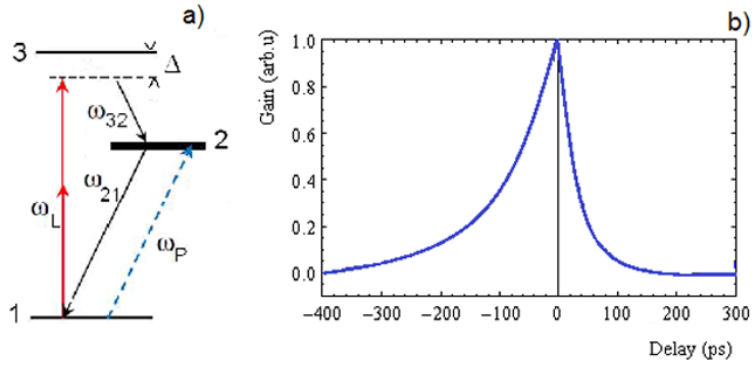

Fig. 3. (a) Schematic of FWDFM in a three-level quantum system: a strong laser pulse excites the two-photon transition at frequency $2\omega_L$ (red arrows online) and a weak probe is injected at the lower one-photon transition at frequency ω_P. (b) FWDFM efficiency versus the delay time τ_L: numerically eveluated rising and decaying signals displaying the difference of relaxation parameters of coherences in one- and two-photon resonantly excited channels (100 ps and 30 ps, respectively).

solution of the Redfield-type equations can be used to solve actual problems of ultrafast spectroscopy of molecular aggregates.

Specifically, we consider the localized many-level system, in which the ground (g) and excited (e) electronic states contain manifolds of vibrational levels $|g_1, g_2,...\rangle$ and $|e_1, e_2,...\rangle$, correspondingly, $g_m(e_m)$ being integer numbers enumerating quantum states in the ground (excited) vibrational manifolds (here, index m enumerates vibrational modes, which we do not specify at the moment). Let us assume two ground state manifolds to be electric-dipole coupled to the corresponding manifolds of vibrational states in excited manifold by the appropriate set of dipole moments with relative values for the given Huang-Rhys S related to the corresponding Franck-Condon (FC) factors as follows [40]:

$$\langle e_n \mid g_m \rangle = \sqrt{\frac{g_m}{e_n}} \exp -\frac{S}{2} S^{\frac{e_n - g_m}{2}} L_{g_m}^{e_n - g_m}(S), \tag{12}$$

where $L_{g_m}^{e_n - g_m}(S)$ is a Laguerre polynomial, and $g_m \le e_n$. For the case $g_m \le e_n$, the following relation holds:

$$\langle e_n \mid g_m \rangle = (-1)^{g_m - e_n} \langle e_m \mid g_n \rangle . \tag{13}$$

Again, as it was described in Section 2, absorption changes are detected by a weak probe field, after the system is exposed to the laser (pump) pulse, of frequency (ω_L) which is considered to be close to resonance with the dominant transition (see Fig. 4) in a molecule, whereas the probe field due to its broad spectrum couples the amount of vibrational states of the ground and excited manifolds, which is sufficient to reproduce both absorption and emission spectra of the molecule. Now the equations for material variables read:

$$\frac{\partial \rho_{ij}^{\mathrm{L}}}{\partial t} = -i\Delta_{ij}^{\mathrm{L}} \rho_{ij}^{\mathrm{L}} - i\sum_{i,j} [\Lambda_{\mathrm{L}} n_{ij}^{0} + \Lambda_{\mathrm{P}} n_{ij}^{-1}] - \sum_{kl} \Re_{ij}^{kl} \rho_{kl}^{\mathrm{L}}, \tag{14a}$$

$$\frac{\partial \rho_{ij}^{\mathrm{P}}}{\partial t} = -i\Delta_{ij}^{\mathrm{L}} \rho_{ij}^{\mathrm{P}} - i\sum_{i,j} [\Lambda_{L} n_{ij}^{1} + \Lambda_{\mathrm{P}} n_{ij}^{0}] - \sum_{kl} \Re_{ij}^{kl} \rho_{kl}^{\mathrm{P}}, \tag{14b}$$

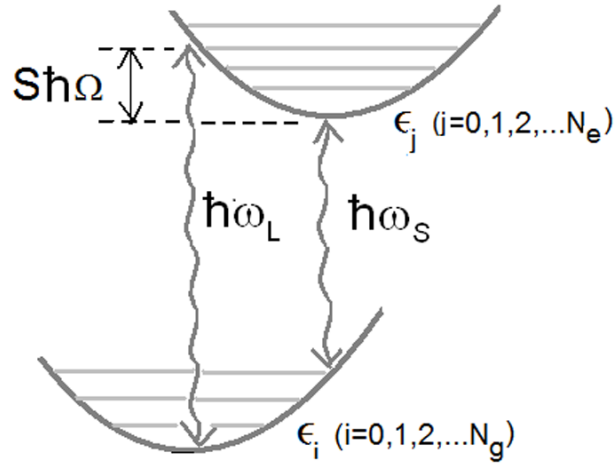

Fig. 4. Schematic of optical transitions between the ground and excited states in a molecule.

$$\frac{\partial \rho_{ii}^{1}}{\partial t} = -2i\sum_{j} \left[\Lambda_{\mathrm{P}} \rho_{ji}^{\mathrm{L}} e^{-i\Delta_{\mathrm{LP}} t} + \Lambda_{\mathrm{L}}^{*}\right] + \sum_{k} \Re_{kk}^{ii} \rho_{kk}, \tag{14c}$$

$$\frac{\partial \rho_{jj}^{1}}{\partial t} = 2i\sum_{i} \left[\Lambda_{\mathrm{P}}^{*} \rho_{ij}^{\mathrm{L}} e^{i\Delta_{\mathrm{LP}} t} + \Lambda_{\mathrm{L}}^{*} \rho_{ji}^{\mathrm{P}}\right] + \sum_{k} \Re_{kk}^{jj} \rho_{kk}^{1}, \tag{14d}$$

$$\frac{\partial \rho_{ii}^{0}}{\partial t} = -2i\sum_{j} \left[\Lambda_{\mathrm{L}} \rho_{ij}^{l} - \Lambda_{\mathrm{P}}^{*} \rho_{ji}^{\mathrm{P}} e^{i\Delta_{\mathrm{LP}} t} - \mathrm{c.c.}\right] + \sum_{k} \Re_{kk}^{ii} \rho_{kk}^{0}, \tag{14e}$$

$$\frac{\partial \rho_{jj}^{0}}{\partial t} = 2i\sum_{i} \left[\Lambda_{\mathrm{L}} \rho_{ji}^{\mathrm{L}} - \Lambda_{\mathrm{P}}^{*} e^{i\Delta_{\mathrm{LP}} t} \rho_{ij}^{\mathrm{P}} - \mathrm{c.c.}\right] + \sum_{k} \Re_{kk}^{jj} \rho_{kk}^{0}, \tag{14f}$$

where $n_{ij} = \rho^{k}_{ii} - \rho^{k}_{jj}$ and R_{ij}^{kl} are the matrix elements of the Redfield tensor, which describes the relaxation process (population as well as polarization relaxation). Here, Eqs. (14a) and (14b) describe the electronic (high frequency) coherences, Eqs. (14c) and (14d) describe the population kinetics, whereas Eqs. (14e) and (14f) describe the dynamics of the coherences, which in case of the vibrational modes are responsible for the low frequency oscillations observed in differential absorption spectra for positive delays [1, 26, 40].

Thus, in our representation, taking into account the one-phonon processes only, the relaxation tensor elements of interest are

$$\Re_{00}^{11}, \quad \Re_{i-1,\,i-1}^{jj}, \tag{15}$$

which are the population transfer within the excited state and ground state manifolds, and index $j(i)-1$ means energy lowering by one quanta within one of the vibrational modes, whereas terms

$$\Re_{ij}^{ij} = \frac{1}{T_2} \tag{16}$$

give the electronic polarization relaxation. Note that according to Eq. (7), a detailed balance between the adjacent transitions holds:

$$\Re_{ii}^{jj} = \frac{\Gamma_{j,i,i,j}^{+} + \Gamma_{j,i,i,j}^{-}}{\Gamma_{i,j,j,i}^{+} + \Gamma_{i,j,j,i}^{-}} = e^{-\frac{\hbar\omega_{i,j}}{kT}}, \tag{17}$$

where $\hbar\omega_{ij}$ is the energy difference between the vibrational substates, and the fundamental relaxation parameters R_0 and T_2 are the only free parameters in the theoretical approach used. Further, for the electronic coherence transfer according to Eq. (15) not only the secular terms ($\Delta\omega = 0$) will be considered, taking into account situations where polarisation frequencies differ by one vibrational quantum ($\Delta\omega = \hbar\Omega$). Specifically, the following elements of the Redfield tensor $\Re_{ji}^{ij}$ fulfilling the relationships: $e_k - e_i = 0, \pm 1$ and $g_l - g_j = 0, \pm 1$, giving $\Re_{i\pm1,j}^{k\pm1,l}$, have to be taken into account. (Recall that here every index *i, j, k, l* denotes compound indexes in manifolds of vibrational states).

For quantitative modelling two vibrational (low and high) frequency modes, namely 30 cm^{-1} and 130 cm^{-1}, were taken into account. The set of Huang-Rhys factors, which determine the strength of the electron interaction with these vibrational modes, was varied. A 3D plot of the calculated DAS versus wavelengths and delay times between pump and probe pulses is shown in Fig. 5 for different sets of the Huang-Rhys factor. Figure 5(a) is depicted with $S = \{0.15, 0.25\}$ for low and high frequency modes, respectively, whereas in Fig. 5(b) the case with $S = \{1.5, 2.5\}$ is shown. The main advantages of our modelling as compared to common perturbative treatments (using e. g. MBO model) developed by describing the femtosecond transient spectra of organic molecules [1] are (i) the explicit description of the excitation through vibrational modes in both the ground and excited states, and (ii) the inclusion of the transfer of electronic and vibrational excitations. The first aspect seems to be more appropriate at a high temperature, as the population of higher vibrational modes in the initial conditions

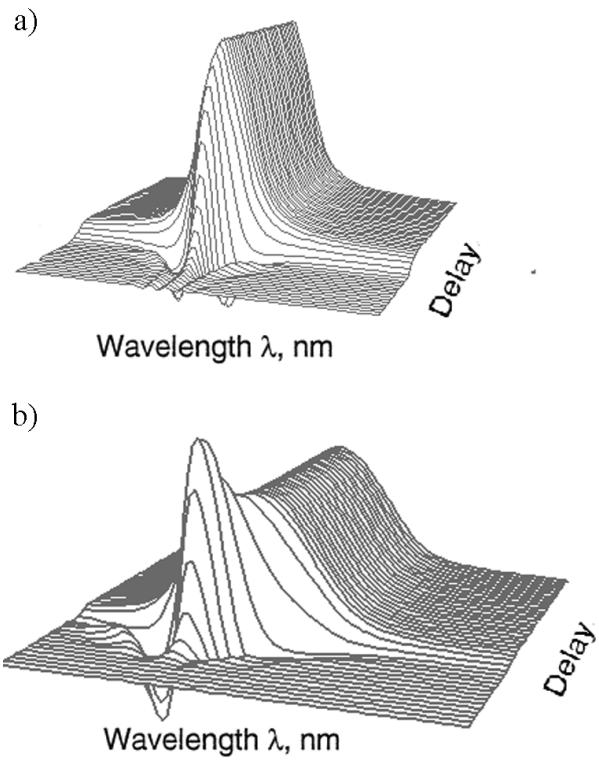

Fig. 5. Three-dimensional plot of the DAS, demonstrating (a) absence and (b) presences of the prominent Stokes shift in a molecule with weak $S = \{0.15, 0.25\}$ and strong $S = \{1.5, 2.5\}$ coupling between electronic and vibrational modes. Relaxation parameters: $T_2 = 20$ ps^{-1}, $R_0 = 50$ ps^{-1}.

strongly influences the correlation function of the vibrational subsystem. The second aspect is crucial in determining the value of the signal bleaching in vicinity around zero delay time, which is caused by the electronic coherence transfer. Indeed, the initial bleaching results from the reduction of the ground state population, and electronic coherence transfer is an important modulation factor of this bleaching. Further in the course of time the relaxation through vibrational states in the excited electronic state takes place. This redistribution expresses itself via the gradual shift of the bleaching band relaxation towards the Stokes-shifted fluorescence band.

The initial oscillating feature (at negative delay times) is evidently due to the pump pulse interaction with the free induction generated by the probe pulse (as it was noticed above considering coherent effects in a 2LQS). On the other hand, oscillations in the spectra for positive time delays

are relatively weak, hidden by the relaxation over vibrational states at room temperature and are not seen in Fig. 5. Nevertheless, oscillations due to the vibrational coherences can be disclosed in our treatment simply by taking pump laser frequency tuned below the dominant transition in the spectra. The calculated DAS for some specific wavelengths are shown in Fig. 6 for the same set of parameters as in Fig. 5, except Δ_L was taken off-resonance from the dominant transition in the molecule, so that population in the excited electronic state becomes negligible. In this case oscillations due to the coherences excited in the vibrational manifold of the ground states are evidently seen in the decay kinetics for positive time delays.

Our treatment provides basic sources for information on vibrational relaxation dynamics as well as electron transfer processes, which can be obtained by fitting experimental and theoretical modelling data.

4. Strong excitation induced effects in molecular aggregates

Molecular aggregates [41] are of practical and theoretical interest because of their specific photophysical and spectroscopic features including huge nonlinearities [42, 43] and excitation transfer phenomena. Now it is well established that collective excitations of the aggregate (one- and two-exciton states) are responsible for the spectral properties

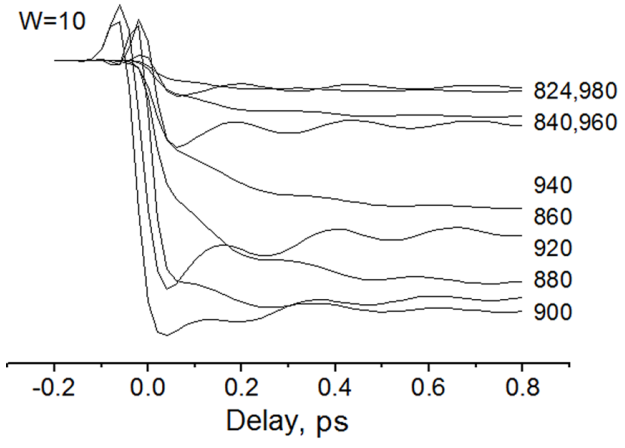

Fig. 6. Calculated difference transmission kinetics with parameters at various wavelengths. S = {1.5, 2.5}. Other parameters as in Fig. 5.

and excitation kinetics in aggregated systems. A number of theoretical and experimental studies (see e. g. [41, 44],) have been devoted to different aspects of this problem.

The formation of the structure of excitonic energy bands appears when distinct transition frequencies of N monomers in an aggregate split due to the resonance interaction into N one-exciton states. Higher two-exciton states can be occupied in a twofold excited segment of an aggregate allowing transitions from the one- to two-exciton band. Accordingly, the transitions between the ground- and one-exciton states lead to positive contributions to the DAS (absorption and ground state bleach), while the transitions between the one- and two-exciton states result in a negative contribution (excited state absorption).

4.1. Annihilation enhanced FWM in molecular J-aggregates

When considering the nonlinear response of molecular aggregates, the crucial importance of exciton–exciton annihilation, as found in [45, 46], should be stressed. The effect becomes of great importance in forming the optical response of the aggregate subsystem as the pump intensity rises. Within the process of exciton–exciton annihilation two colliding excitons annihilate creating one twofold excited state, i. e. a state of the second excitonic energy manifold. This state relaxes to the first manifold very fast, and the excess energy is distributed over vibrational degrees of freedom.

As an example which demonstrates the importance of exciton–exciton annihilation in laser spectroscopy of molecular aggregates (and possible photonic devices), we present here results on computer modelling of transient degenerate FWM which take into account both the saturation and annihilation processes [47]. In our model it was assumed that relaxation from the second excitonic manifold appears faster than annihilation itself, so that the rate of the whole process is determined by the annihilation rate in good approximation. In this case it is not necessary to include the second manifold into the consideration. Using the full semiclassical description of light and matter interaction, in close analogy with that presented in the background section, we account for the interplay of nonlinear effects at high pump intensities. In this case significant enhancement of the FWM efficiency

in the region of saturation due to the annihilation processes of excitons can be demonstrated. The analysed contribution of annihilation to intensity and wavelength dependence of the DFWM signal (see Fig. 7) was found to be in good qualitative agreement with experimental findings of DFWM at the excitonic resonance in J-aggregates of pseudoisocyanine chloride (PIC) [48].

4.2. Ultrafast pump-probe spectroscopy of strongly excited linear aggregates

It was demonstrated in the previous section that exciton–exciton annihilation effects become of great importance in forming the optical response of the molecular aggregate subsystem as the pump intensity rises. Additionally, due to the dependence of nonlinearity in J-aggregates on the coherence length (the number of molecules over which the excitation is delocalized), annihilation and the amount of disorder in the aggregated chains affect the optical response. Moreover, both processes are closely related to each other: the annihilation constant in the aggregate exhibits the dependence on the (mean) coherence length and, again, energy degradation processes (after the annihilation event) may result in inhomogeneity changes, which reduce the coherence length. All these changes of disorder strongly affect the aggregate spectra, being dependent on the eigenfunctions, eigenvalues and optical transition strengths in the quantum system.

Assuming that the molecules of an ensemble of aggregates exhibit strong inter-molecular interactions (in comparison to molecular–bath interactions) we will describe aggregate excitations in terms of the well-known fermionization model [49–51]. It was noticed above that the linear spectra of such a media are known to be formed from collectivized eigenstates in N excitonic manifolds (see e. g. [52, 53]). Further we will use this approach and perform our study on two excitonic manifolds of one-dimensional chains. When taking into account the nearest-neighbour interaction of the molecules, the eigenvalues of the collectivized states in these manifolds for perfectly ordered (homogeneous) linear aggregates are given by the simple expressions [21, 51, 54]. But even under ideal preparation conditions the meso-aggregate chain never becomes ideal and contains a certain number of rotated molecules and molecular segments. This so-called "static" disorder reduces to a certain amount the delocalization of excitation or, in other words, the length within the aggregate. The spectra of disordered aggregates were analysed previously by the perturbative procedure in [55] and by the direct numerical diagonalization [56] of the interaction Hamiltonian with the (static) site energy disorder.

In fact, for the line shape analysis of a disordered linear aggregate one should deal with the Hamiltonian H_0 of the form

$$H_0 = \sum_{m=1}^{N}\sum_{n=1}^{N} H_{mn}\,|l\rangle\langle m|, \tag{18}$$

where $H_{mn} = (\langle\in\rangle + D_n)\delta_{m,n} + J_{n,m}$ and summation runs over the possible one-molecule excitations $|n\rangle$ of the aggregate, $\langle\in\rangle$ stands for the average molecular excitation energy, D_n is the offset energy of the nth molecule, and J_{nm} is the inter-molecular interaction between molecules n and m.

Even for strong excited aggregates the interaction Hamiltonian H_{int} can be considered a small perturbation. In this case the eigenvalues and eigenvectors for the particular realization of the disorder can be found by diagonalizing the matrix H_{nm} numerically. Then kth eigenvalue $\in_k$ gives the energy of the eigenstate, whereas the corresponding eigenvector specifies its wave function in k-space: $|k\rangle = \sum_n \phi_{kn}\,|n\rangle$. Again, expanding the density matrix operator within this new basis of the wave functions in k-space the equations for material variables according to Eqs. (1–3) may be written down.

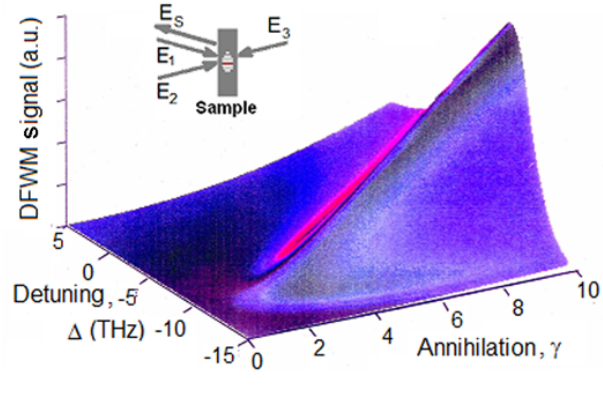

Fig. 7. 3D plot of the DFWM signal versus detuning from resonance Δ and annihilation constant γ.

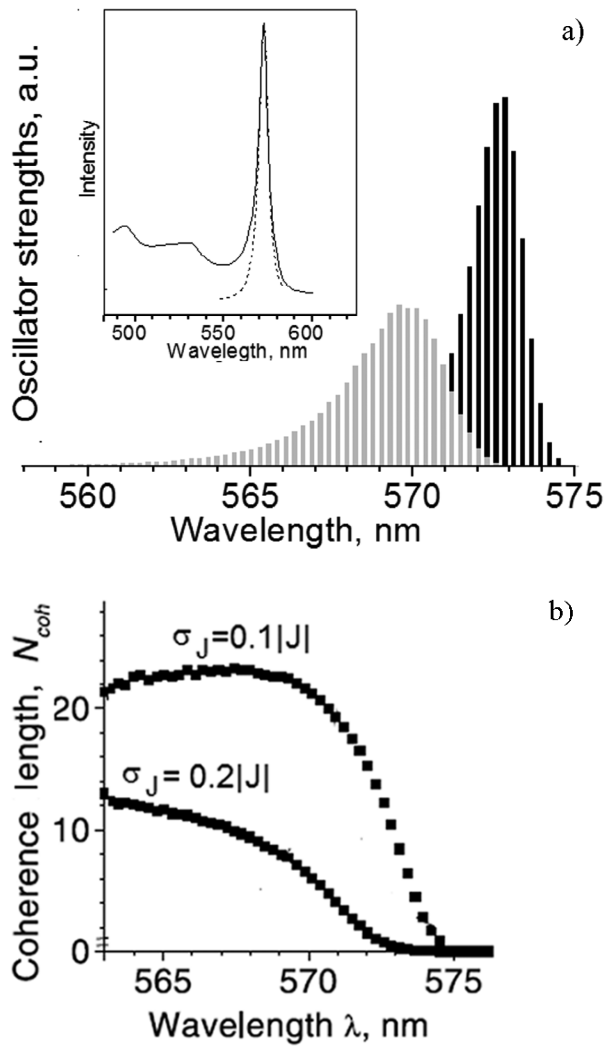

Fig. 8. (a) Stick spectra of the aggregate ensembles with different amount of off-diagonal disorder: $\sigma_J = 0.20 \times |J|$ (gray columns) and $\sigma_J = 0.10 \times |J|$ (black columns). $|J| = 600$ cm^{-1} × 50000 realizations of disorder calculated for the aggregate chains consisting of $N = 100$ monomers. In the inset the experimentally measured J-band (solid line) of the PIC aggregates and evaluated numerically (dashed line). (b) Numerically evaluated exciton coherence length N_{coh} dependences for both cases.

Inconsistence of the perturbative treatment of the energy spectra of the aggregate is also seen from Fig. 8(a), where the stick spectra as obtained by numerical diagonalization of the Hamiltonian matrix $N = 100$ of an aggregate for the two particular sets (σ_E, σ_J) of the standard deviations and the intermolecular interaction {0.1 × |J|, 0.1 × |J|} and {0.1 × |J|, 0.2 × |J|} are shown. It is seen from this figure that the eigenvalue-shift overcomes the energy offsets between the neighbouring eigenvalues, i. e. validity of perturbation approximation for evaluation of the aggregate spectra is not ensured.

It is also instructive to evaluate the corresponding delocalization (coherence) length N_{coh} [56, 57]:

$$N_{coh}^{k} = N\rho(\in_k)/\langle\sum_{j=1}^{N}\delta(\in_k - \in_j)\sum_{n=1}^{N}\phi_{j,n}^{4}\rangle, \qquad (19)$$

where $\rho(\in_k)$ stands for the density of quantum states. Appropriate coherence lengths calculated for cases considered above are depicted in Fig. 8(b). It is seen that the main contribution to the aggregate spectra of interest is given from segments of 5–10 molecules. It should be pointed out that the above-described treatment allows us not only interpret the dependent spectra of the aggregate as contributed from the combined action of exciton–exciton annihilation and subsequent dynamic disordering processes, but also gives a possibility to interpret the transient stages of the aggregate exhibiting e. g. lasing due to the excess off-diagonal disorder. For this purpose two aggregate ensembles with a different amount of disorder were considered by deriving appropriate equations [54]. The population redistribution between these aggregates was included by different relaxation rates from the two-fold excited state of the initial aggregate to the manifold of one-exciton states of the additionally disordered one. The last one is assumed to have no population prior to excitation (as described by the initial condition). In this case the calculation procedure, as above, involves the numerical diagonalization of the matrix $\hat{H}_{n,m}$ for the certain number (10000 in our calculations) of disorder realizations and kinetics of the material variables is determined as an average of density matrix elements over these realizations.

As it follows from the results presented in Fig. 10, certain relations between rates of excitation annihilation and relaxation in the system lead to transient stages exhibiting the feature to lasing in a strongly excited aggregate ensemble.

4.3. Annihilation probed exciton delocalization in molecular aggregates

Finally, we present the heuristic approach for estimating exciton delocalization by using pump-probe absorption spectroscopy data. The idea behind

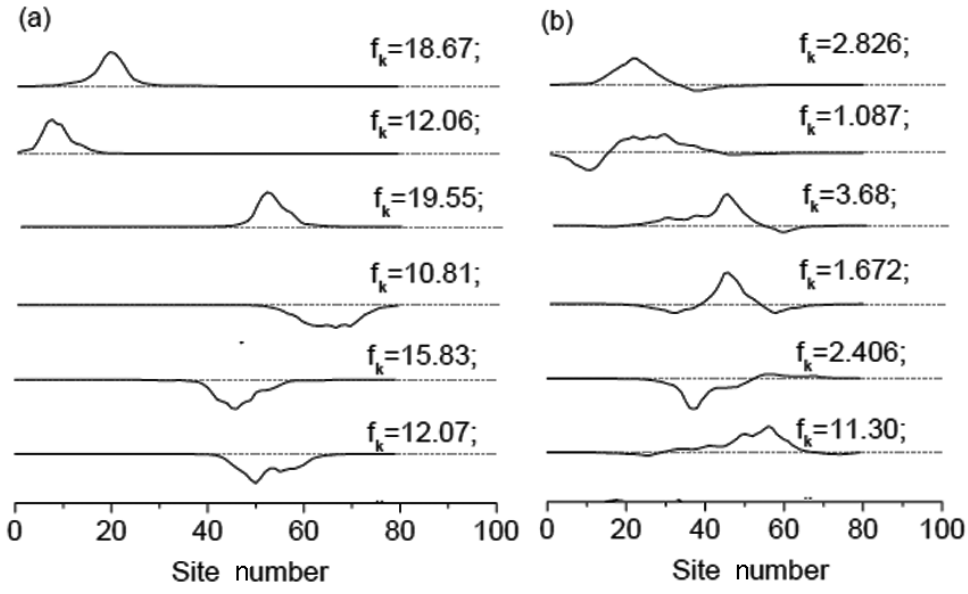

Fig. 9. Typical realizations of the low-energy eigenfunctions k 1 and 5 of the J-aggregate ensembles depicted for the set of the standard deviations $\sigma_J = 0.20 \cdot |J\}$ and $\sigma_E = 0.10 \cdot |J|$ of the matrix elements H_{mn}. Each plot also shows the corresponding state oscillator strength f_k in units of the oscillator strength of the individual molecule.

this approach is to explore the migration-limited character of the exciton–exciton annihilation in molecular aggregates. For the sake of brevity we will illustrate it for the one-dimensional regular molecular aggregates only while the extension of this approach for the aggregates of arbitrary topology will be published elsewhere.

It has been shown that at high excitation intensities the asymptotic pump-probe kinetics of aggregates is dominated by the exponential decay [58]. This component represents the first passage time for the last pair of excitons. The exact analytical expression for the smallest eigenvalue of this pairwise annihilation component τ_a^{-1} can be easily obtained from the spectral representation of the migration-limited excitation trapping problem by taking into account the hopping twice as fast as the excitation. In case of periodic boundary conditions (ring topology) of the aggregate it reads [58, 59]:

$$\tau_a^{-1} = 8 \sin^2(\pi/2N) / \tau_h, \tag{20}$$

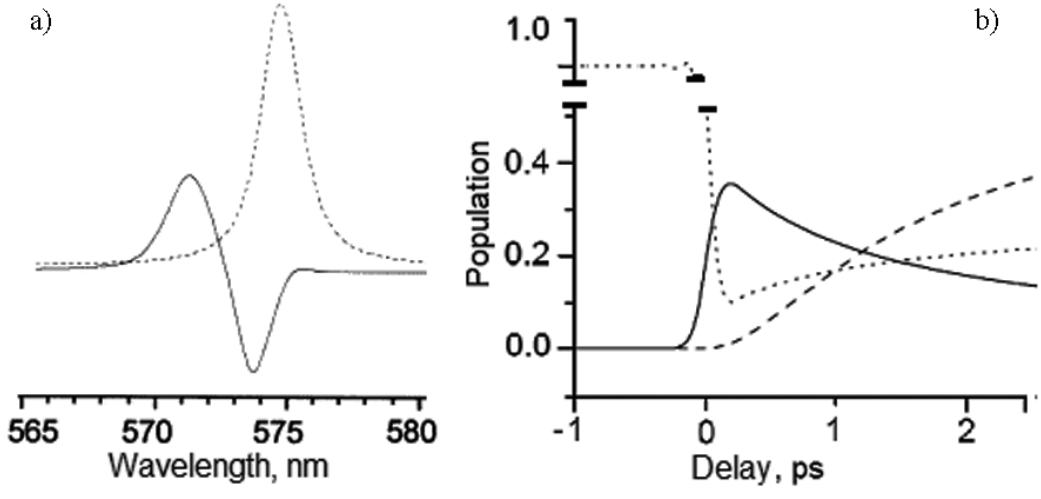

Fig. 10. (a) Aggregate spectra at delay time τ = 2 ps (solid line) and initial spectra of the aggregate (dashed line). Blue shifted emission is produced here by induced excess disorder in the aggregate ensemble after exciton–exciton annihilation. (b) Population kinetics in excited aggregate ensemble: ground state (dotted line), first manifold of the excited states (dashed line), second manifold of the excited states (solid line).

where N is the number of hopping sites in the aggregate, and τ_h is an exciton hopping time. It should be noted that the following lifetime expression for migration determined anisotropy decay of polarized aggregate excitation [60],

$$\tau_d = \tau_h/8 \sin^2(\pi/2N), \quad (21)$$

provides complementary relation between hopping time and the number of hopping sites explored during random walk on a ring. The latter parameter provides information on the exciton delocalization. For instance, the bacterial light-harvesting complex LH2 from the photosynthetic bacteria Rh. *sphaeroides* contains a ring aggregate of closely packed 18 bacteriochlorophyll molecules. The measured constants $\tau_a = 0.59$ ps and $\tau_d = 0.1$ ps [58] substituted to Eqs. (20) and (21) result in the hopping time $\tau_h = 0.27$ ps and $N = 6.6$ sites. It is therefore expected that the localized exciton is spanned over $N_{coh} = 18/N = 2.8$ bacteriochlorophyll molecules. This view of coherent exciton hopping over different localization sites on the LH2 aggregate has recently been obtained while simulating fluorescence kinetics of a single LH2 complex from Rps. *acidophila* [61]. Additionally, the approach has already been used while analyzing exciton coherence in the bacterial light harvesting complex LH1 and reaction center of Photosystem II, thin film and crystalline C60, as well as conjugate polymers [59]. Recently, it has also been used while studying artificial light-harvesting aggregates of porphyrin [62–65].

5. Conclusions

In this paper, motivated by the recently discovered significance of the quantum coherences in light harvesting efficiency [9], we have demonstrated the suitability of the Redfield theory for the nonperturbative description of different examples of ultrafast pump-probe spectroscopy of atomic, molecular and aggregated systems, with special attention paid to the lifetime of electronic coherences. Particularly, for the specific model of transient DAS of the two-level system it was concluded that definite phase relations between induced in 2LQS coherences and light field (accounted for in non-Markovian approach) results in a distinct time dependent shift of the DAS bleaching. Applying this description, which is based on numerical analysis of the Redfield-type equations, to three- and many-level quantum systems, the possibilities for tracing coherences in difference FWM experiments as well as exciton–exciton annihilation enhanced FWM in molecular aggregates were discussed. The method allows one to follow excitation dynamics over the vibrational states during the time of excitation and signatures of the excited coherences in ultrafast pump-probe spectroscopy. Finally, the given possibilities to observe lasing due to the exciton–exciton annihilation as well as estimate coherence length in molecular aggregates were discussed.

We conclude that nonperturbative treatment of the Redfield equations is suitable for many experimental situations of ultrafast FWM spectroscopy, from atoms to artificial molecular aggregates and photosynthetic complexes, simulating both de-coherence and coherence transfer effects.

References

[1] Sh. Mukamel, *Principles of Nonlinear Optical Spectroscopy* (Oxford University Press, New York–Oxford, 1995).

[2] J. Mompart and R. Corbalan, Lasing without inversion, J. Opt. B Quant. Semiclass. Opt. **2**(3), R7 (2000).

[3] M.M. Kash, V.A. Sautenkov, A.S. Zibrov, L. Hollberg, G.R. Welch, M.D. Lukin, Y. Rostovtsev, E.S. Fry, and M.O. Scully, Ultraslow group velocity and enhanced nonlinear optical effects in a coherently driven hot atomic gas, Phys. Rev. Lett. **82**, 5229–5232 (1999).

[4] D.F. Phillips, A. Fleischhauer, A. Mair, R.L. Walsworth, and M.D. Lukin, Storage of light in atomic vapor, Phys. Rev. Lett. **86**, 783–786 (2001).

[5] D.S. Bradshaw and D.L. Andrews, Optically controlled resonance energy transfer: Mechanism and configuration for all-optical switching, J. Chem. Phys. **128**(14), 144506 (2008).

[6] E. Biolatti, R.C. Iotti, P. Zanardi, and F. Rossi, Quantum information processing with semiconductor macroatoms, Phys. Rev. Lett. **85**(26), 5647–5650 (2000).

[7] P. Chen, C. Piermarocchi, and L.J. Sham, Control of exciton dynamics in nanodots for quantum operations, Phys. Rev. Lett. **87**(6), 067401 (2001).

[8] A. Nazir, B.W. Lovett, and G.A.D. Briggs, Creating excitonic entanglement in quantum dots through the optical Stark effect, Phys. Rev. A **70**, 052301 (1986).

[9] G.S. Engel, T.R. Calhoun, E.L. Read, T.-K. Ahn, T. Manal, Y.-C. Cheng, R.E. Blankenship, and G.R. Fleming, Evidence of wavelike energy transfer

through quantum coherence in photosynthetic systems, Nature **446**, 782–786 (2007).
[10] V. Butkus, D. Abramavicius, A. Gelzinis, and L. Valkunas, Two-dimensional optical spectroscopy of molecolar aggregates, Lith. J. Phys. **50**(3), 267–303 (2010).
[11] D. Abramavicius, V. Butkus, and L. Valkunas, Interplay of exciton coherence and dissipation in molecular aggregates, in: *Quantum Efficiency in Complex Systems II: From Molecular Aggregates to Organic Solar Cells*, Vol. 85, eds. U. Wurfel, M. Thorwart, and E.R. Weber (Elsvier Academic Press, San Diego, 2011) pp. 3–46.
[12] A. Gelzinis, D. Abramavicius, and L. Valkunas, Non-Markovian effcts in time-resolved fluorescence spectrum of molecular aggregates: Tracing polaron formation, Phys. Rev. B **84**(24), 245430 (2011).
[13] V. Butkus, A. Gelzinis, and L. Valkunas, Quantum coherence and disorder-specific effects in simulations of 2D optical spectra of one-dimensional J-aggregates, J. Phys. Chem. A **115**(16), 3876–3885 (2011).
[14] V. Butkus, D. Zigmantas, L. Valkunas, and D. Abramavicius, Vibrational vs. electronic coherences in 2D spectrum of molecular systems, Chem. Phys. Lett. **545**, 40–43 (2012).
[15] V. Butkus, L. Valkunas, and D. Abramavicius, Molecular vibrations-induced quantum beats in two-dimensional electronic spectroscopy, J. Chem. Phys. **137**(4), (2012).
[16] T. Meier, V. Chernyak, and S. Mukamel, Femtosecond photon echoes in molecular aggregates, J. Chem. Phys. **107**(21), 8759–8774 (1997).
[17] D. Abramavicius and S. Mukamel, Chirality-induced signals in coherent multidimensional spectroscopy of excitons, J. Chem. Phys. **124**(3), (2006).
[18] K. Blum, *Density Matrix Theory and Applications* (Plenum Press, New York, 1981).
[19] Y.R. Shen, *The Principles of Nonlinear Optics* (John Wiley & Sons, New York, 1984).
[20] E. Gaizauskas and L. Valkunas, Femtosecond four-wave mixing spectroscopy of molecular aggregates, J. Phys. Chem. B **101**(37), 7321–7326 (1997).
[21] E. Gaižauskas and K.-H. Feller, Effects of strong excitation induced disorder on pump-probe spectra of molecular aggregates, J. Lumin. **102–103**, 13–20 (2003).
[22] C.P. Slichter, *Principles of Magnetic Resonance* (Springer Verlag, New York, 1990).
[23] N. Raja, S. Reddy, P.A. Lyle, and G.J. Small, Applications of spectral hole burning spectroscopies to antenna and reaction center complexes, Photosynth. Res. **31**, 167–194 (1992).
[24] G. Small, Spectral hole burning: Methods and applications to photosynthesis, in: *Biophysical Techniques in Photosynthesis*, eds. J. Amesz and A.J. Hof (Kluver Academic Publishers, 1996) pp. 123–136.
[25] W.T. Pollard and R.A. Friesner, Solution of the Redfield equation for the dissipative quantum dynamics of multilevel system, J. Chem. Phys. **100**, 5054–5065 (1993).
[26] M. Chachišvilis and V. Sundström, Femtosecond vibrational dynamis and relaxation in the core light-harvesting complex of photosynthetic purple bacteria, Chem. Phys. Lett. **261**, 165–174 (1996).
[27] E. Gaižauskas and L. Valkunas, Coherent transients in 2-level approximation, Opt. Commun. **109**(1–2), 75–80 (1994).
[28] E. Gaižauskas, A. Beržanskis, and K.-H. Feller, Effects of non-Markovian relaxation in the femtosecond differential absorption spectroscopy, Chem. Phys. **235**(1–3), 123–130 (1998).
[29] A. Savickas and E. Gaižauskas, Manifestation of the optical Stark effect in differential transmission spectra, Lith. J. Phys. **48**(2), 155–162 (2008).
[30] J.-Y. Bigot, M.T. Portella, R.W. Schoenlein, C.J. Bardeen, A. Migus, and C.V. Shank, Non-Markovian dephasing of molecules in solution measured with three-pulse femtosecond photon echoes, Phys. Rev. Lett. **66**, 1138–1141 (1991).
[31] E. Gaizauskas, K.H. Feller, and L. Valkunas, Manifestation of the transition from the excited state by means of femtosecond four-wave mixing spectroscopy, Opt. Quant. Electron. **28**, 1203–1213 (1996).
[32] A. Guzman de Garcia, P. Meystre, and R.R.E. Salomaa, Time-delayed probe spectroscopy in two-photon–pumped systems, Phys. Rev. A **32**, 1531–1540 (1985).
[33] E. Gaižauskas and G. Gedvilas, Theory of coherent one- and two-photon interaction in a three-level system, Opt. Commun. **91**(34), 312–320 (1992).
[34] C.S. Mullin, D. Kim, M.B. Feller, and Y.R. Shen, Picosecond studies of optical second harmonic generation in atomic vapor, Phys. Rev. Lett. **74**, 2678–2681 (1995).
[35] O. Kittelmann, J. Ringling, A. Nazarkin, G. Korn, and I.V. Hertel, Direct observation of coherent medium response under the condition of two-photon excitation of krypton by femtosecond UV-laser pulses, Phys. Rev. Lett. **76**, 2682–2685 (1996).
[36] A. Nazarkin, G. Korn, O. Kittelmann, J. Ringling, and I.V. Hertel, Femtosecond-pulse two-photon resonant difference-frequency mixing in gases: a technique for tunable vacuum-ultraviolet femtosecond-pulse generation and a spectroscopic tool for studying atoms in strong laser fields, Phys. Rev. A **56**, 671–684 (1997).
[37] I. Pop and L. Moorman, Electromagnetically induced generation, gain in delayed wave mixing, and measuring coherent states using

quantum-interference windows, Phys. Rev. A **60**, 678–686 (1999).
[38] E. Gaižauskas, D. Pentaris, T. Efthimiopoulos, and V. Vaicaitis, Probing electronic coherences by combined two- and one-photon excitation in atomic vapors, Opt. Lett. **38**, 124–126 (2013).
[39] M. Chachišvilis, H. Fidder, and V. Sundström, Electronic coherence in pseudo two-collour pump-probe spectroscopy, Chem. Phys. Lett. **234**, 141 (1995).
[40] J.A. Leegwater, Theory of coherent oscillations in the photosynthetic reaction center, J. Phys. Chem. **99**(29), 11605–11611 (1995).
[41] *J-aggregates*, ed. T. Kobayashi (World Scientific, Singapore, 1996).
[42] E. Hanamura, Rapid radiative decay and enhanced optical nonlinearity of excitons in a quantum well, Phys. Rev. B **38**, 1228–1234 (1988).
[43] E. Hanamura, Very large optical nonlinearity of semiconductor microcrystallites, Phys. Rev. B **37**, 1273–1279 (1988).
[44] H. Van Amerongen, L. Valkunas, and R. Van Grondelle, *Excitons* (World Scientific, Singapore, 2000).
[45] V. Sundstrm, T. Gillbro, R.A. Gadonas, and A. Piskarskas, Annihilation of singlet excitons in J aggregates of pseudoisocyanine (PIC) studied by pico- and subpicosecond spectroscopy, J. Chem. Phys. **89**, 2754–2762 (1988).
[46] H. Stiel, S. Daehne, and K. Teuchner, J-aggregates of pseudoisocyanine in solution: New data from nonlinear spectroscopy, J. Lumin. **39**(6), 351–357 (1988).
[47] E. Gaižauskas, K.H. Feller, and R. Gadonas, Anihillations enhanced 4-wave mixing in molecular aggregates, Opt. Commun. **118**(3–4), 360–366 (1995).
[48] R. Gadonas, K.-H. Feller, A. Pugzlys, G. Jonusauskas, J. Oberle, and C. Rulliere, Wavelength and intensity-dependent transient degenerate four-wave mixing in pseudoisocyanine J-aggregates, J. Chem. Phys. **106**(20), 8374–8383 (1997).
[49] D.B. Chesnut and A. Suna, Fermion behavior of one-dimensional excitons. J. Chem. Phys. **39**, 146 (1963).
[50] G. Juzeliūnas, Exciton absorption spectra of optically excited linear molecular aggregates, Z. Phys. D **8**, 379–384 (1988).
[51] G. Juzeliūnas and P. Reineker, Influence of exciton–exciton interaction on one-to-two exciton transitions in molecular aggregates with linear and circular geometries, J. Chem. Phys. **107**(23), 9801–9806 (1997).
[52] F.C. Spano, J.R. Kuklinski, and S. Mukamel, Temperature-dependent superradiant decay of excitons in small aggregates, Phys. Rev. Lett. **65**, 211–214 (1990).
[53] F.C. Spano, J.R. Kuklinsky, and S. Mukamel, Cooperative radiative dynamics in molecular aggregates, J. Chem. Phys. **94**, 7534 (1991).
[54] E. Gaizauskas and K.-H. Feller, Nonlinear transients to pump-probe spectra of strongly excited J-aggregates, Opt. Commun. **216**(1–3), 217–224 (2003).
[55] E.W. Knapp, Lineshapes of molecular aggregates, exchange narrowing and intersite correlation, Chem. Phys. **85**, 73–82 (1984).
[56] H. Fidder, J. Knoester, and D.A. Wiersma, Optical properties of disordered molecular aggregates: A numerical study, J. Chem. Phys. **95**(11), 7880 (1991).
[57] D.J. Thouless, Electrons in disordered systems and the theory of localization, Phys. Rep. **13**(3), 93–142 (1974).
[58] G. Trinkunas, J.L. Herek, T. Polivka, V. Sundstrom, and T. Pullerits, Exciton delocalization probed by excitation annihilation in the light-harvesting antenna LH2, Phys. Rev. Lett. **86**(18), 4167–4170 (2001).
[59] G. Trinkunas, Probing of molecular aggregates with exciton annihilation, J. Lumin. **102**, 532–535 (2003).
[60] J.A. Leegwater, Coherent versus incoherent energy transfer and trapping in photosynthetic antenna complexes, J. Phys. Chem. **100**(34), 14403–1440 (1996).
[61] R. van Grondelle and V.I. Novoderezhkin, Quantum effects in photosynthesis, in: *22nd Solvay Conference on Chemistry – Quantum Effects in Chemistry and Biology*, Vol. 3, eds. G.R. Fleming, G.D. Scholes, and A. DeWit (Elsevier Science BV, Amsterdam, the Netherlands, 2011).
[62] R.A. Jensen, R.F. Kelley, S.J. Lee, M.R. Wasielewski, J.T. Hupp, and D.M. Tiede, Fast energy transfer within a self-assembled cyclic porphyrin tetramer, Chem. Commun. **16**, 1886–1888 (2008).
[63] M.-C. Yoon, S. Cho, P. Kim, T. Hori, N. Aratani, A. Osuka, and D. Kim, Structural dependence on excitation energy migration processes in artificial light harvesting cyclic zinc(II) porphyrin arrays, J. Phys. Chem. B **113**(45), 15074–15082 (2009).
[64] Ch. Maeda, P. Kim, S. Cho, J.K. Park, J.M. Lim, D. Kim, J. Vura-Weis, M.R. Wasielewski, H. Shinokubo, and A. Osuka, Large porphyrin squares from the self-assembly of *meso*-triazole-appended L-shaped *meso-meso*-linked Zn-II-triporphyrins: Synthesis and efficient energy transfer, Chem. Eur. S. **16**(17), 5052–5061 (2010).
[65] J. Yang and D. Kim, Excitation energy migration processes in various multi-porphyrin assemblies, Phil. Trans. R. Soc. A **370**(1972), 3802–3818 (2012).

KOHERENTINIŲ KVANTINIŲ BŪSENŲ PAIEŠKA ULTRASPARČIĄJA LAZERINE SPEKTROSKOPIJA

E. Gaižauskas [a], G. Trinkūnas [b]

[a] *Vilniaus universiteto Lazerinių tyrimų centras, Vilnius, Lietuva*

[b] *Valstybinis mokslinių tyrimų institutas Fizinių ir technologijos mokslų centras, Vilnius, Lietuva*

Santrauka

Autoriai, remdamiesi moksline patirtimi ir atliktais darbais, apžvelgia koherentinės medžiagos bei lauko sąveikos ypatumus bei apraiškas, stebimas ultrasparčiosios žadinimo-zondavimo spektroskopijos metodais. Aptariami šios technikos privalumai siekiant nustatyti atomuose, molekuliniuose agregatuose bei biologiniuose dariniuose sužadintų koherentinių būsenų gesimo ir pernašos kelius, taip pat galimybės įvertinti tokių sužadinimų gyvavimo trukmę bei koherentiškumo ilgį, plotą ar tūrį (kai kalbama apie molekulinius agregatus). Aprašant lazerinės žadinimo-zondavimo spektroskopijos matavimus remiamasi tankio matricos, užrašytos atomo, molekulės ar eksitoninių funkcijų bazėje, evoliucijos skaitmeniniu sprendimu (netaikant trikdžių teorijos artinių elektromagnetinio lauko ir kvantinių medžiagos būsenų sąveikai aprašyti).